THE JOURNAL OF PHYSICAL CHEMISTRY C

Article

pubs.acs.org/JPCC

Redox Modification of CdSe–ZnS–Polymer Quantum Dots: Photoassisted Fluorescence Quenching and Recovery

X. X. Yu,[†,‡] J. N. Li,[‡] K. C. Kwok,[‡] M. C. Paau,[§] Martin M. F. Choi,[§] K. K. Shiu,[§] J. Y. Chen,*[,†] and N. H. Cheung*[,‡]

[†]State Key Laboratory of Surface Physics and Department of Physics, Fudan University, Handan Road 220, Shanghai 200433, China

[‡]Department of Physics, Hong Kong Baptist University, Kowloon Tong, Hong Kong, China

[§]Department of Chemistry, Hong Kong Baptist University, Kowloon Tong, Hong Kong, China

Supporting Information

ABSTRACT: Commercial CdSe–ZnS–polymer quantum dots (QDs) were shown to be readily quenched by strong oxidants such as potassium permanganate. When exposed to permanganate solution of millimolar concentration for hours, damage was severe and the QDs would be permanently bleached. When oxidant concentration was micromolar and reaction time was minutes, oxidation would be mild and bleached QDs could recover their fluorescence if the oxidant was removed and the QDs subsequently irradiated. Light was essential in activating the fluorescence recovery. Light could also transform mild oxidations into severe ones if administered with the oxidant simultaneously. A model of the bleaching and recovery was proposed. It was based on the oxidative attack of the Zn–ligand bond and its repair. The model helped explain the critical role that light played and was consistent with all the experimental observations. By means of photocatalyzed oxidation of single QDs, a redox probe of high spatial and temporal resolution was demonstrated.

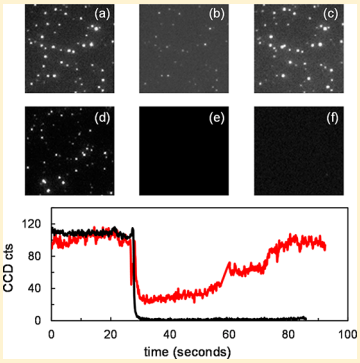

INTRODUCTION

Semiconductor quantum dots (QDs) have drawn much attention because of their superior photophysical properties relative to organic dyes. For example, their absorption spectra are broader, and their absorption cross sections are 1–2 orders of magnitude bigger; their emission bands are narrower and tunable, and they are much more photostable.[1,2] For the purpose of biolabeling, QDs are generally grafted covalently with amphiphilic ligands. This ensures colloidal and chemical stability and enables solubility and biocompatibility.[3] It also passivates the QD surface by removing defect sites. Trapping of excitonic charge is therefore prevented, and radiative recombination is favored. If the QD–ligand bond is broken, defects will appear and fluorescence will be quenched. Such was shown to occur when QDs were treated with strong oxidizing agents such as potassium permanganate[4] or mild oxidants if the reaction was photoenhanced.[5]

To improve the photo and chemical stability, the QD core can be capped with a wider band gap material to confine the electrons and holes. An example is a ZnS shell around a CdSe core,[6] which is less easily oxidized than the core-only version.[7] However, core–shell QDs were still bleached by strong oxidants such as hydrogen peroxide.[8] An additional protective measure is cross-linking the ligands with a polymer layer.[9] This further passivates the QD surface. Such kind of CdSe–ZnS–polymer QDs are available commercially.[a] They are widely adopted for biolabeling and fluorescence microscopy. Nevertheless, their sensitivity to redox agents had not been investigated. More generally, the constancy of the fluorescence signal of core–shell–polymer QDs under various chemical environments has to be established before quantitative interpretation of the fluorescence images can be reliably drawn.

There are yet more interesting reasons for studying the redox properties of QDs. Although QDs may become photounstable when modified by redox agents, this apparent disadvantage can be turned to good use. For example, bleaching of CdSe–ZnS QDs by hydrogen peroxide could be exploited to measure the oxidant concentration.[8] Bleaching of CdTe QDs by potassium permanganate could be reversed by reducing agents. As a result, oxidation-sensitized QDs could be used to probe reducing agents such as vitamin C.[4] Furthermore, redox modification not only produced redox probes, it is also a means to control light-induced charge transfer from the QD to a proximal acceptor, and novel applications in photovoltaics and photodynamic therapy were demonstrated.[10,11]

Clearly, the use of QDs in biolabeling is widespread, and their applications in photoinduced charge transfers and in chemical probing are emerging. Whether CdSe–ZnS–polymer QDs have a special role to play in this regard is the general question we want to address. At the same time, we want to answer two specific questions. First, is bleaching a deterministic dimming of all dots or the stochastic extinction of some dots?[12,13] Second, what is the role played by light in the redox reaction? Most studies did not identify photons as a key

Received: May 9, 2012
Revised: July 26, 2012
Published: August 2, 2012

   dx.doi.org/10.1021/jp304494t | J. Phys. Chem. C 2012, 116, 18479–18486

player.[4,8,14] However, for a range of QDs, light was shown to activate and accelerate the oxidative bleaching and recovery process.[5,15,16] We therefore carried out systematic investigation of the redox modifications of CdSe−ZnS−polymer QDs. In particular, we paid special attention to three aspects of the process: (1) the separate role of chemicals and light and their synergy, (2) the kinetics of the reaction, and (3) the redox effects at the ensemble as well as the single dot level.

EXPERIMENTAL DETAILS

Chemicals and Standard Assays. The CdSe−ZnS−polymer quantum dots were purchased from Invitrogen (Qdot Biotin Conjugates Qdot 655). All other chemicals were analytical reagent grade. Purified water (Milli-Q water, >18 MΩ cm^{-1}) was used as blank solvent.[b]

For scanning purpose, redox modifications of QDs were conducted in 96-well plates. The steady-state fluorescence intensities were measured on a microplate reader (Tecan Infinite 200). Absorption spectra of the QDs at various stages of the redox reaction were measured on a microvolume spectrophotometer (NanoDrop ND 1000). Oxidized QDs were analyzed by a capillary electrophoresis system (Beckman MDQ).

Flow Cell Assembly. Kinetics experiments were performed in flow channels mounted on a prism-coupled total internal reflection (TIR) fluorescence microscope (Olympus IX-71). The setup is shown schematically in Figure 1. It was based on

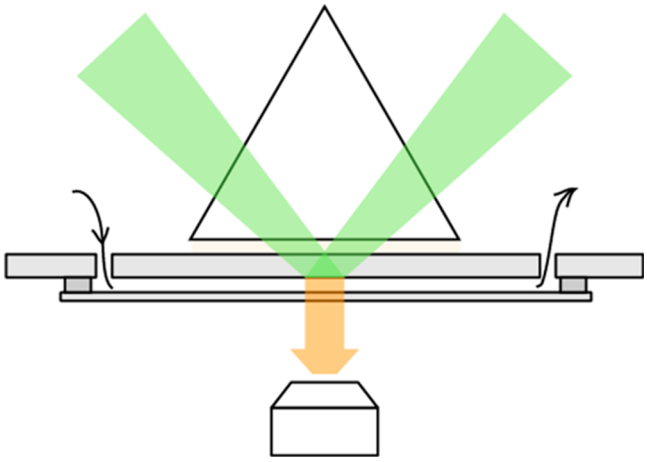

Figure 1. Schematics of the experimental setup. The flow channel was formed by a quartz slide on top and a coverglass below. Reagents were flowed in and out through ports on the slide. QDs were tethered on the underside of the slide. They were excited by the evanescent light of a laser beam that was totally internally reflected. Fluorescence emissions were collected through a microscope objective.

one of our earlier designs.[17] The instrumentation details were reported elsewhere.[17,18] Briefly, the flow channel was a quartz slide sealed with cover glass. Liquid inflow and outflow were from the top. The underside of the quartz slide was coated with positively charged poly(L-lysine) (PLL). Negatively charged QDs were electrostatically tethered on the PLL surface. The tethering was firm and could withstand multiple flushes of reagents. The QD coating density could be varied by controlling the concentration of the QD solution during coating. Dense and sparse coatings were respectively used for ensemble and single dot studies.

Tethered QDs were excited by the evanescent waves of a TIR laser beam that was incident through a quartz prism. The laser beam was TE polarized (s-wave). Either 532 or 473 nm laser wavelength was used. The laser beam power was adjustable and was monitored on power meters (OPHIR Nova, Newport 1815-C). The fluorescence signal was collected either through a 10× NA 0.25 or an oil immersion 60× NA 1.42 microscope objective. The collected light was band-filtered and directed through a polarizing beam splitter. The parallel and perpendicularly polarized images were captured with an electron-multiplied CCD (Andor iXon) operating in movie mode.

Oxidative Bleaching and Recovery. In a typical oxidation experiment, the tethered QDs in a water-filled channel were first illuminated with the laser beam. A movie of the fluorescent dots was continuously taken while $KMnO_4$ solution was flowed into the channel. The entire decay process of the QD fluorescence was captured. Under some conditions, the bleached QDs could recover their fluorescence. To monitor the recovery, fluorescence of unbleached QDs was recorded to give the initial brightness. With the laser beam blocked, oxidizing agents were then flowed in to oxidize and bleach the QDs, followed by injection of water to flush out the reagents. Finally, with the laser beam on, the entire course of photoactivated fluorescence recovery was video recorded. Specific details of each experiment were given in the next section, either in the main text or in the corresponding figure captions.

Data Processing. Movies in TIF format were analyzed with MATLAB programs. In ensemble measurements, each frame generally featured two bright patches corresponding to the parallel and the perpendicular polarization. For each patch, the background-subtracted pixel intensities were averaged over the area of interest to give the QD intensity I for that polarization. The total intensity is defined as $I_{total} = I_{\parallel} + 2I_{\perp}$.[19] Fluorescence anisotropy (FA) is defined as $FA = (I_{\parallel} - I_{\perp})/I_{total}$.[19] As will be explained in the next section, the time courses of I_{total} and FA were useful in elucidating the bleaching and recovery mechanisms. Single dot movies were processed in a similar way. However, because of the limited signal-to-noise ratio, background subtraction had to be treated more carefully. For a given dot, we used a nearby blank region as its background.[20,21]

RESULTS AND DISCUSSION

Oxidative Bleaching. To study how the various redox agents affect the QD fluorescence, reactions were conducted in 96-well plates. The fluorescence change was measured with a microplate reader. Four reducing agents—β-mercaptoethanol (BME), sodium borohydride ($NaBH_4$), sodium azide (NaN_3), and dithiothreitol (DTT)—were used. They changed the fluorescence by no more than 20% even at concentrations up to 100 μM. Oxidizing agents H_2O_2, HNO_3, and $KMnO_4$, however, had much stronger effects; fluorescence brightness was halved at oxidant concentrations of only about 10 μM. $KMnO_4$ was the strongest among the three.

It is well-known that light may enhance the bleaching process.[5] In order to study the respective effect of oxidant, light, and their combination, we did our subsequent experiments in a flow cell with tethered QDs (Figure 1). Reagents could be flowed in or flushed out at will. We used $KMnO_4$ as the oxidant for maximal effect. The QDs were excited by the evanescent light waves of a total internally reflected laser beam. Background interference was therefore negligible.

We first gauged the extent of photobleaching without $KMnO_4$. The sample cell was filled with water, and the QDs were irradiated continuously. Two QD coating densities were tried: singles at 3×10^6 dots/cm^2 and ensembles at 8×10^{11} dots/cm^2. In both cases, fluorescence was found to be unchanged when irradiated continuously at 1.8 W cm^{-2} for 3 min.

We then measured the extent of photoenhanced oxidative bleaching in the presence of $KMnO_4$. A typical experimental run was as follows. The camera was turned on, and 20 μM permanganate solution was injected into the sample cell while the QDs were irradiated with a 532 nm laser. In a few seconds, the reagents would reach the QDs under view and their fluorescence would decay. We took movies of the fluorescence decay at different laser powers. Results of two power settings, 62 mW cm^{-2} (light blue solid curve) and 1.6 W cm^{-2} (dark blue curve) are shown in Figure 2. The start of the decay was defined as time zero. As can be seen, the decays were fast. Brightness was halved in 0.4 and 0.2 s for the respective cases. The highest power density we used was 2.6 W cm^{-2} (data not shown), but the bleaching rate was similar to the 1.6 W cm^{-2} case. We believe this limiting rate was due to reagent mixing rather than quenching kinetics.[c]

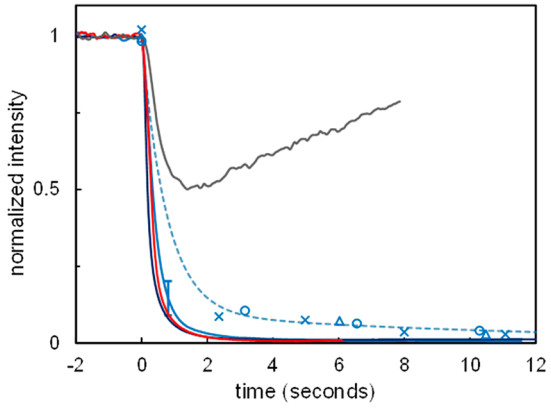

Figure 2. Oxidative bleaching of QDs by potassium permanganate. Shown are the normalized fluorescence intensities as functions of time for various combinations of oxidant concentration and 532 nm irradiance: 20 μM at 1.6 W cm^{-2} (dark blue trace) and 62 mW cm^{-2} (light blue trace), or without light (blue data points, with blue dotted trend line); 5 μM at 1.6 W cm^{-2} (red trace); and 400 nM at 1.6 W cm^{-2} (gray curve). The injected permanganate solution reached the QDs under view at t = 0. The standard deviation of three separate measurements is shown as error bar for one representative case.

As the laser power was reduced, bleaching would be slower. The slowest rate corresponding to the zero-light limit could be measured by blocking the laser beam except for brief fluorescence measurements at selected time points.[d] The results are shown in Figure 2 (○, △, and ×) together with the trend line (light blue dotted curve). As can be seen, the half-life in the dark limit was about 0.6 s.

At a lower permanganate concentration of 5 μM, the quenching rate was found to be slightly lower than the 20 μM case (Figure 2, red curve). At a still lower oxidant concentration of 400 nM, the bleaching was not only slower but the QDs soon recovered their brightness (Figure 2, gray curve). This trend reversal could be explained by the fact that the oxidant concentration of 400 nM was comparable to the effective QD concentration and the permanganates might be used up. We will return to this point in the next section.

On the basis of the above findings, we could conclude that QDs mixed with excess $KMnO_4$ in the dark would be quenched in seconds. Adding light would hasten the quenching to fraction of seconds although light alone hardly photobleached the QDs.

We measured the absorbance of the QDs at 532 and 473 nm. We found no significant (<±5%) change be they bleached with or without light. We also measured their fluorescence anisotropy (FA) during the bleaching process. There was an insignificantly small increase of about 15 mA and then a gradual decrease to the original value. Both absorption and anisotropy results seem to indicate that oxidation affected the emission but not the excitation of the QDs.[22,23] More absorption, anisotropy and microplate reader results are plotted in Figures S1−S4 of the Supporting Information.

Photoactivated Recovery. As mentioned previously, bleached QDs could recover when the oxidants were depleted. We investigated this recovery process. We bleached QDs in the flow cell with 20 μM permanganate solution for 2 min in the dark. We then flushed the cell with multiple injections of water to remove the permanganates. The QDs were then irradiated with laser light of various powers and wavelengths. Fluorescence was shown to reappear. The recovery trend could be satisfactorily fitted by the function $I(t)$

$$I(t) = \frac{A}{1 + \left(\frac{\tau}{t}\right)^n} \tag{1}$$

where the amplitude A, the half-life τ, and the exponent n were fitting parameters. We found that the amplitude A was about the same as the fluorescence brightness before the bleaching, indicating that the recovery was practically 100%. By dividing the fluorescence data with A, the normalized intensities for various laser irradiances and wavelengths could be plotted on the same graph for easy comparison as shown in Figure 3. The three green curves were produced with a 532 nm beam at the respective irradiance of 1700, 45, and 12 mW cm^{-2}, as labeled. The fitting curve (eq 1) for the 45 mW cm^{-2} is also shown to illustrate the goodness of fit. As can be seen, higher irradiance induced faster recovery. We determined τ for many more irradiances. A plot of $1/\tau$ versus 532 nm irradiance is shown in the inset of Figure 3 (green circles). The recovery rate $1/\tau$ could be modeled with an exponential function (green dashed curve)

$$\frac{1}{\tau}(p) = \frac{1}{\tau_0}\left[1 - \exp\left(-\frac{p}{p_0}\right)\right] \tag{2}$$

where the asymptotic rate $1/\tau_0$ was set to 0.3 s^{-1} and the characteristic irradiance p_0 was fixed at 420 mW cm^{-2}.

We also tested 473 nm laser irradiation. One recovery curve at 42 mW cm^{-2} is shown in Figure 3 (dark blue curve). As can be seen, the recovery was faster than the 532 nm case of comparable power density. The dependence of the recovery rate on 473 nm irradiance is plotted in the inset, together with the functional fit based on eq 2 (blue triangles and dashed line). The asymptotic rate $1/\tau_0$ was again set to 0.3 s^{-1} like the 532 nm case. However, the characteristic irradiance p_0 was 7 times lower, at 60 mW cm^{-2}.

In summary, light played a crucial role in the fluorescence recovery of permanganate-bleached QDs, in the following ways. First, light activated the recovery process. Without light, the

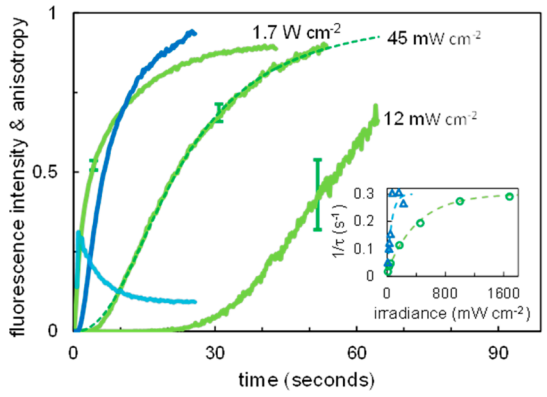

Figure 3. Photoactivated recovery of dark-bleached QDs. Plotted is the normalized fluorescence intensity against irradiated time at three 532 nm irradiance of 1700, 45, and 12 mW cm^{-2} (green curves). Each trace is the average of three sets of data; the representative standard deviations are shown as error bars. All experimental traces could be satisfactorily fitted by $I(t) = A/[1 + (\tau/t)^n]$; they were then divided by A to give the normalized intensity. One such fit was shown for the 45 mW cm^{-2} case. Shown also is the recovery activated by 473 nm laser at 42 mW cm^{-2} (dark blue curve), together with its corresponding change in fluorescence anisotropy (light blue curve). Inset is a plot of the recovery rates against irradiance for 532 nm (green ○) and 473 nm (blue △) laser irradiation. Measurement error was about the size of the data symbols. Trend lines are based on eq 2.

bleached QDs would remain dark. We had stored bleached dots in water in the sample cell for 40 min, and they remained dark. Second, stronger irradiation revived the fluorescence proportionally faster, until the limiting rate of 0.3 s^{-1} was reached. Third, 473 nm photons revived the fluorescence 7 times faster than 532 nm photons, although the extinction coefficient was only 1.7 times higher.[24]

We mentioned that the polarization anisotropy (FA) of the QD fluorescence did not change significantly during the bleaching process. Here, we monitored FA during the recovery process. A typical result, for the case of 473 nm irradiation at 42 mW cm^{-2}, is shown in Figure 3 (light blue curve). Data for the initial 0.6 s was not shown because the signal was too weak for anisotropy to be well-defined. As can be seen, FA increased sharply at first, peaked at about 310 mA, and then gradually dropped at rates similar to the recovery of fluorescence. The final anisotropy value measured was about 90 mA, which approached the 80 mA of unbleached QDs. We will discuss the meaning of the anisotropy change in a later section.

We also wondered if the recovered QDs would stay bright if polarization ε of the incident laser beam was rotated. To investigate this, we changed the illumination from total internal reflection to normal incidence to allow easy rotation of ε. Recovered QDs stayed equally bright as ε was rotated through 90°. This loss of ε memory will be interpreted later. More photoactivated recovery results are plotted in Figure S5 of the Supporting Information.

Oxidative Damage. We saw that QDs bleached with 20 μM permanganate for 2 min in the dark could recover their fluorescence completely when photoactivated. In this section, we studied the recovery of QDs that were bleached more extensively. For longer bleaching times, such as 5 h, only 70% of the original fluorescence was recovered. When the permanganate concentration was increased to 1 mM, less than half recovered if bleached for 20 s, and none recovered if bleached for 5 h. The results of this kind of permanent oxidative damage are plotted in Figure 4 for the respective case of bleaching with 20 μM (black □) and 1 mM (red ×)

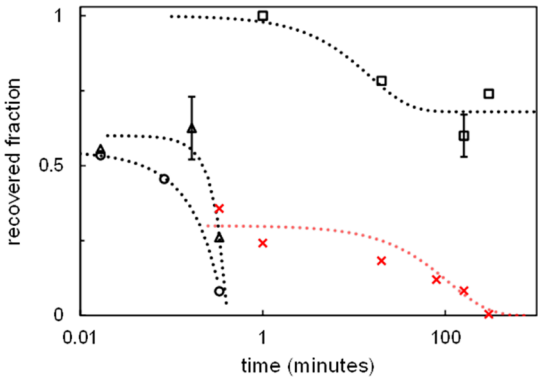

Figure 4. Fluorescence recovery of bleached QDs. The fraction finally recovered was plotted against reaction time. Shown are cases of 20 μM [$KMnO_4$] and 532 nm irradiance of zero (□), 160 (△), and 910 mW cm^{-2} (○) as well as 1 mM [$KMnO_4$] without irradiation (red ×). Dotted curves are trend lines. Representative uncertainties are shown as error bars.

$KMnO_4$. The bleaching time (x-axis) is shown in log scale. As can be seen, while 1 mM could be very destructive, 20 μM was only mildly destructive even for hours of bleaching.

However, if the 20 μM permanganate bleaching was photoenhanced with 532 nm laser light, the damage was orders of magnitude faster and more extensive. This is shown in Figure 4 for the respective case of 160 (△) and 910 mW cm^{-2} (○). As can be seen, only about half of the fluorescence intensity could be recovered if irradiated for only a few seconds. That recovered fraction dropped to about 10% when 473 nm laser light was used (not shown in Figure 4; see Figure S6 of Supporting Information).

Clearly, photons played an enhancement role in the oxidative damage of QDs. To see if the photodamaged QDs would remember the excitation ε, we again used normal incidence and rotated ε through 90°. The damaged QDs remained dark throughout.

Single Dots Analysis. We reported the fluorescence recovery of QD ensembles. Here, we studied the recovery process at the single dot level by sparsely tethering the QDs and took movies of numerous single dots. A typical image is shown in Figure 5 (top inset). The QDs were bleached in 20 μM permanganate for 2 min in the dark. After flushing out the oxidant, they were activated at t = 0 by 532 nm light at 2 W cm^{-2}. The time courses of the fluorescence of selected dots are shown in Figure 5 (lower two insets). Both gradual and stepwise recoveries were observed.[e]

Based on the trajectory of each QD, the dot brightness averaged over a particular time interval could be computed. For example, for the upper and lower trajectory shown in the inset, the average brightness in the time interval 0−0.8 s was 2 and 0 ccd counts, respectively. In a similar way, we computed the brightness of 284 single dots. We plotted their brightness distribution in Figure 5 (red curve). Clearly, these dots were dim at this initial stage. At a later stage, from 0.8 to 2.6 s, the distribution (green curve) shifted to higher ccd counts, indicative of fluorescence recovery. At a still later time, 10.2−12.8 s, the distribution (light blue curve) shifted further to the right and overlapped almost perfectly with the brightness distribution of unoxidized QDs (dark blue curve). Apparently,

dx.doi.org/10.1021/jp304494t | J. Phys. Chem. C 2012, 116, 18479−18486

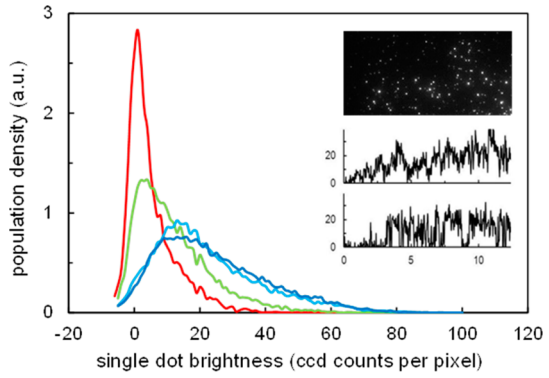

Figure 5. Photoactivated recovery of single QDs. Plotted is the population density against dot brightness at various stages of recovery: 0–0.8 s (red), 0.8–2.6 s (green), and 10.2–12.8 s (light blue). The brightness distribution of untreated QDs is also shown (dark blue). Because of background subtraction, some pixels carried negative counts. Top inset is a typical movie frame showing the perpendicularly polarized image. Bottom inset shows the trajectories of two representative dots undergoing photoactivated fluorescence recovery with the *y*-scale in ccd counts and *x*-scale in seconds. 532 nm laser at 2.03 W cm^{-2} was used.

the fluorescence recovery was not only complete at the ensemble level; it was also complete at the single dot level in the sense that each single QD recovered its full brightness.

We also studied cases when single QDs were bleached more extensively and recovery was only partial. We found the recovered singles still regained their full brightness while those that did not recover remained totally dark. In other words, at the single dot level, recovery was an all-or-none process. This observation was consistent with the theoretical model that accounted for the change in transition rate between a bright and a dark state upon proton or charge transfer.[25]

Plausible Model. The detailed structure of the commercial QDs is proprietary, but brief descriptions are available in the vendor's literature.[24] These QDs were probably prepared in hydrophobic solvents with the ZnS shell coated with phosphine-based ligands. These hydrophobic ligands were subsequently made water-soluble by one of two methods: adsorption of amphiphilic polymers or exchange by thiols with polar ends.[26,27] The most likely end group was COO^-.

The two plausible structures are depicted in Scheme 1. In both cases, the ~3 nm diameter CdSe core was surrounded by a ~1 nm thick ZnS shell, the outside of which was covered with ligands that had carboxyl end groups. The COO^- groups of some ligands were cross-linked by amine-terminated polymers. The CdSe–ZnS type I structure confined the holes within the core. In contrast, the electrons had a finite chance to appear at the ZnS surface.[28] The polymer layer passivated the ZnS surface to remove defect sites and hence prevented electrons from being trapped.[9] Electrons and holes of exciton pairs were therefore unlikely to be separated. Their radiative recombination led to high fluorescence quantum yield. At the same time, the cross-linking via peptide bonds produced a chemically stable polymer shield.[9]

A plausible model of the permanganate oxidation of QD is as follows. The MnO_4^- ion diffused through the polymer coating to attack the Zn–ligand bond by breaking either the Zn–O dative bond (Scheme 1a) or the Zn–S bond (Scheme 1b).[5] The products were $-Zn^+$ on the ZnS shell and a dangling ligand. The dangling ligand would not come off because it was cross-linked. The $-Zn^+$ now acted as an electron trap to cause exciton charge separation, and fluorescence was therefore quenched.[13,29]

Photoenhancement of the oxidative bleaching could be explained this way. The photoproduction of excess electrons transformed the Zn–ligand site into an electron donor;[30] it was thus more readily oxidized. Conversely, when the permanga-

Scheme 1. Two Plausible Structures of QDs[a]

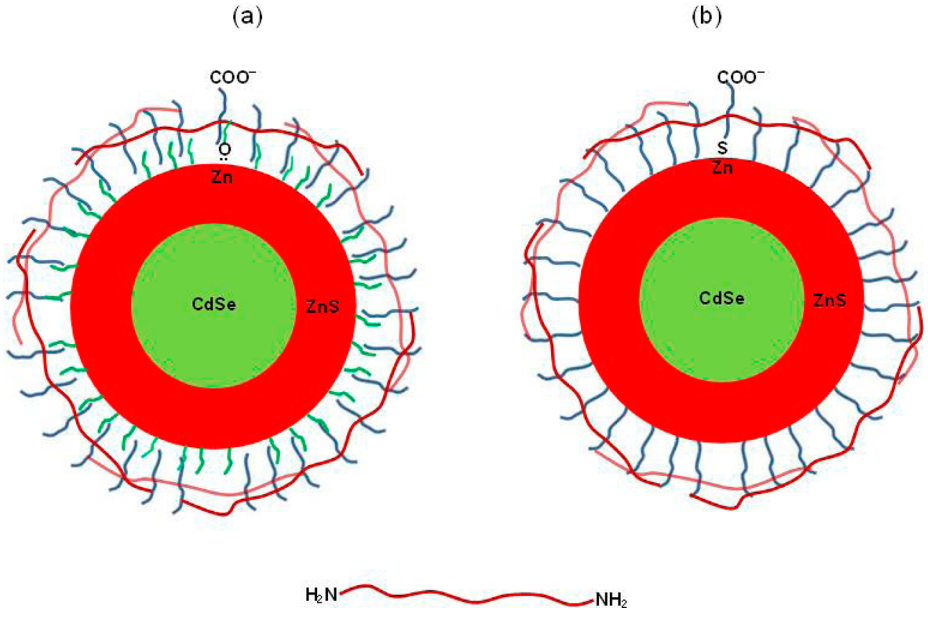

[a]Both had CdSe core (green) with ZnS shell (red) coated with COO^- ligands (blue) cross-linked by amine-terminated linkers (brown). One structure had COO^- terminated amphiphilic polymers adsorbed on hydrophobic phosphine-based coating (a). The other had the phosphine ligands exchanged with COO^- terminated thiols (b). For clarity, only one ligand is labeled in each case. Biotin tethers are not shown.

nate was flushed out, photoinduced electron donation to the Zn^+–dangling ligand site would undo the oxidation step to remake the Zn–ligand bond. This would explain the photoactivated recovery.[15]

Previously, we described the observation of high anisotropy of 310 mA that eventually relaxed to 90 mA during photoactivated recovery (Figure 3, light blue curve). That could be understood this way. With the trapping of photogenerated electrons at the Zn^+ sites, the electron–hole separation would significantly distort the symmetry of the dipole moment of the QD.[22,23] The limiting anisotropy value for tethered fluorophores with collinear excitation and emission dipoles was 400 mA.[19] The observed 310 mA of oxidized QDs suggested that their originally 3D spherical excitation dipole and 2D circular emission dipole were now closer to 1D. When the Zn–ligand bonds were gradually repaired, the electron traps were removed and the dipole symmetry was thus restored. At this point, all memory of the direction of polarization ε of the excitation light should be lost, as was observed.

When oxidation was more extensive and enough Zn–ligand bonds were broken, the entire cross-linked group of ligands might come off. This would cause irreparable damage, and fluorescence could not be recovered, regardless of ε of the excitation light. At the same time, the charge and hydrodynamic mobility of the QD would likely be changed, which should be detectable by capillary electrophoresis.[11]

We recorded the electropherograms of QDs prepared under three different conditions: (1) unoxidized as control, (2) dark oxidation in excess $KMnO_4$ for several minutes, and (3) photoenhanced oxidation for minutes or dark oxidation for hours. The second condition corresponded to mild oxidation when the fluorescence of the QD could be recovered. The third condition corresponded to damaged QDs whose fluorescence was irrecoverable. The results are shown in Figure 6. As can be seen, QDs treated under the second condition (yellow trace) migrated at about the same time as that of the unoxidized ones (red and gray traces). The signal intensities were also similar. In contrast, QDs treated under the third condition (purple, blue, and green traces) showed much weaker signal at t = 6 min, indicative of significant loss of intact QDs. Presumably, damaged QDs migrated at different speed or were lost.[f] Meanwhile, another species migrating at $t \sim 7$ min was observed. The peak was sharp, indicative of homogeneous solutes that were likely to be the detached ligands.

Potential Applications. We demonstrated the bleaching of CdSe–ZnS–polymer QDs by strong oxidants such as potassium permanganate. We showed that the fluorescence of bleached QDs could be recovered when activated by light. However, for QDs that were immersed in oxidants for a long time or if the oxidation was light-enhanced, fluorescence was not recoverable. Our results suggest that, in the presence of strong oxidants, the chemical and photostability of these QDs would be adversely affected. Their use as luminescent labels would be compromised.

Interestingly, oxidative bleaching could be exploited to transform QDs into redox probes.[8] Because light played a critical role in the bleaching and recovery process, the excellent spatial and temporal resolution of the laser beam would be an added advantage. We explored this possibility by taking movies of tethered single quantum dots exposed transiently to oxidants as 20 μL of $KMnO_4$ solution was flushed through the sample cell. Image sequence for permanganate concentration of 400 nM is shown in the top row of Figure 7, corresponding to three

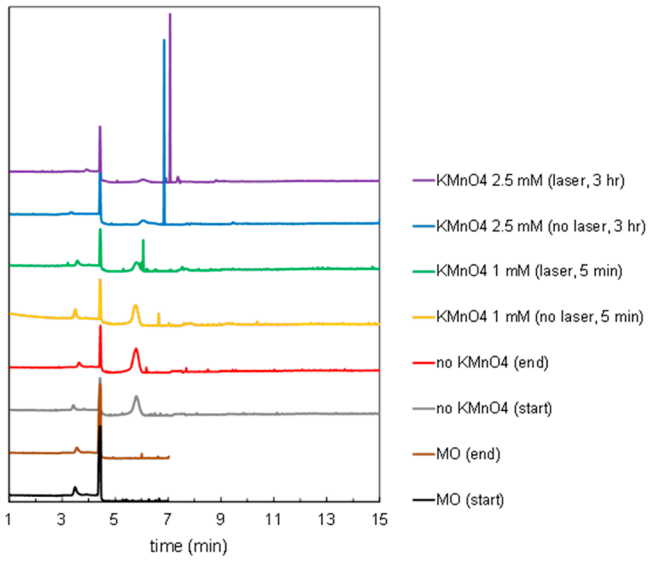

Figure 6. Capillary electrophoresis of QDs treated under various conditions. Plotted is 210 nm absorption against migration time. Bottom two traces (black and brown) were neutral markers mesityl oxide (MO) taken at the beginning and at the end of the run. Next two traces (gray and red) were QDs in phosphate buffered saline without $KMnO_4$, again taken at the beginning and end of the experiment. Next trace (yellow) was QDs treated with 1 mM $KMnO_4$ for 5 min in the dark. The top three traces were QDs bleached extensively: 3 h immersion in 2.5 mM $KMnO_4$ plus 5 min laser irradiation (purple), the same as the last case except without laser irradiation (blue), and 5 min immersion in 1 mM $KMnO_4$ together with laser irradiation (green). All traces were offset vertically, and the neutral markers were lined up for easy viewing.

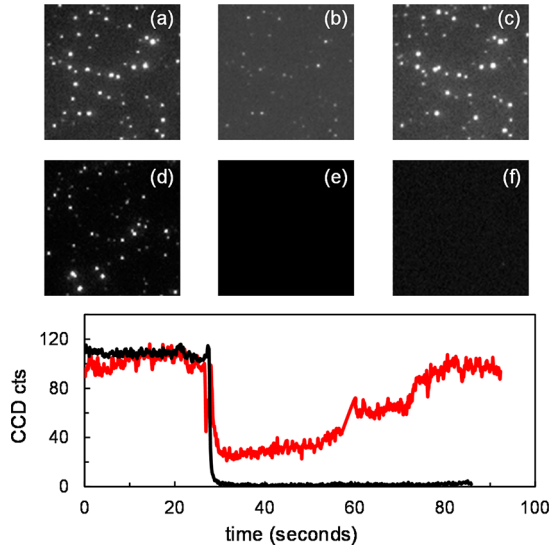

Figure 7. Transient oxidation of single QDs. QDs were sparsely tethered on the substrate for single dot imaging. At t = 27 s, 20 μL of $KMnO_4$ solution was injected into the flow cell that was irradiated with 532 nm light at 1.6 W cm^{-2}. At t = 34 s, reagents were flushed out with water. Top row: sequence of perpendicularly polarized images for [$KMnO_4$] = 400 nM, before permanganate injection (a), just before blank flush (b), and 63 s after blank flush (c). Middle row: equivalent image sequence (d–f) for [$KMnO_4$] = 20 μM. Bottom panel: plot of average single QD brightness as functions of time.

time points, before the injection of $KMnO_4$ (a), prior to blank flush (b), and 1 min after the blank flush (c). The transient

dx.doi.org/10.1021/jp304494t | J. Phys. Chem. C 2012, 116, 18479–18486

bleaching and subsequent recovery was apparent. The second row of images shows analogous events for permanganate concentration of 20 μM. This time the permanent damage was clearly observed. In the bottom panel, we plotted the average dot brightness of single QDs for the two cases as functions of time. As can be seen, the arrival of the permanganate solution could be precisely determined both spatially and temporally. The oxidant concentration could be estimated from the extent of the recovery. We should also point out that subdiffraction-limit imaging of bright fluorophores was well demonstrated.[31] It might be possible to probe redox reactions with nanometer resolution by single dot imaging.

We found that the QDs were not only oxidant probes, but reductant probes as well.[4] This is because dark-bleached QDs recovered faster in reducing agents. This is shown in Figure 8

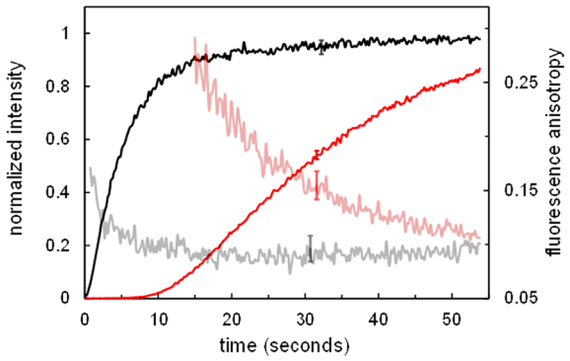

Figure 8. Effect of DTT on photoactivated fluorescence recovery. Plotted are the intensity recovery curves (left-hand *y*-axis) at 0 μM (red) and 4 μM (black) of DTT as well as the corresponding fluorescence anisotropy relaxation curves (pink and gray) using the right-hand *y*-axis. Each displayed curve was the average of three or more data sets. The typical standard deviations are shown as error bars.

when dark-bleached QDs were activated by 532 nm light at 29 mW cm^{-2}, in the absence (red curve) and presence (black curve) of 4 μM DTT. The reducing agent DTT shortened the recovery half-time from 30 to 5 s. The corresponding change in fluorescence anisotropy (FA) is also plotted in Figure 8 (pink and gray curves, right-hand *y*-axis); its faster relaxation in DTT is evident. It should be pointed out that the FA signal was self-normalized. It therefore served as a convenient cross-check of the fluorescence signal.

CONCLUSION

In summary, commercial CdSe−ZnS−polymer QDs were shown to be readily quenched by strong oxidants such as potassium permanganate. Oxidation could be mild or severe. An example of severe oxidation was exposure to 1 mM $KMnO_4$ for hours when the QDs were permanently bleached. In contrast, QDs mildly oxidized by exposure to 20 μM $KMnO_4$ for a few minutes could recover their fluorescence if the oxidant was removed and the QDs subsequently irradiated. Light was essential in activating the recovery of bleached dots; it could also turn mild oxidations into severe ones if administered with the oxidant simultaneously.

We hypothesized that mild and recoverable oxidation was the breaking of isolated Zn−ligand bonds that remained dangling because of the cross-linking and were thus repairable whereas severe oxidation was extensive breaking of Zn−ligand bonds that led to ligand removal on a massive scale. The model was consistent with the results of capillary electrophoresis as well as the all-or-none fluorescence recovery of single QDs.

Photoinduced electron transfer from the CdSe core to the ZnS surface site could then explain the catalytic role that light played in the oxidation damage as well as the fluorescence recovery of bleached QDs. Trapping of electrons at the Zn−ligand broken bond sites caused charge separation. That could explain the quenching as well as the polarization anisotropy of the fluorescence.

Because quenching and recovery were photocatalyzed and clearly visible even at the single dot level, a redox probe of high spatial (tens of nanometers) and temporal (fraction of second) resolution was feasible. It would be interesting to use these readily available QDs as starting material, engineer their electrochemical properties by simple redox modifications, and explore applications that exploit their photoinduced redox sensitivity and electron-transfer functionality.

ASSOCIATED CONTENT

Supporting Information

Further experimental results of the redox of CdSe−ZnS−polymer QDs include (1) the effects of various reducing and oxidizing agents on fluorescence, (2) the absorbance of oxidized QDs, (3) the time course of fluorescence anisotropy during oxidative bleaching and photoinduced recovery, (4) the photoenhanced oxidation at 532 vs 473 nm, and (5) the effect of pH. This material is available free of charge via the Internet at http://pubs.acs.org.

AUTHOR INFORMATION

Corresponding Author

*E-mail: jychen@fudan.edu.cn (J.Y.C.); nhcheung@hkbu.edu.hk (N.H.C.).

Notes

The authors declare no competing financial interest.

ACKNOWLEDGMENTS

This work was supported by the Faculty Research Grant of Hong Kong Baptist University and the General Research Fund of the Research Grant Council of Hong Kong under Grant HKBU 200609. X.X.Y. and J.Y.C. thank the financial support from the National Natural Science Foundation of China (11074053 and 31170802).

ADDITIONAL NOTES

[a]For example, Invitrogen Qdot Nanocrystals from Invitrogen Corp., Grand Island, NY.

[b]We did not use pH buffers because we found that some reagents in pH buffers reacted with $KMnO_4$. With purified water as solvent, we observed that the pH values of the redox solutions used in our experiments were still relatively stable, at 5.6 ± 0.3. More details of the effect of pH on QD oxidation are given in Table S1 and Figures S6 and S7 of the Supporting Information.

[c]When solution of oxidant was injected into the flow cell of pure water, the fluid front would be diluted. The width of this mixed front was about a few millimeters. The flow speed of the fluid was about 2.5 cm s^{-1}. It took about 100 ms for the mixed front to pass.

[d]Fluorescence intensity was based on the first two frames (0.14 s total exposure) of the 1 s movie taken of each previously

unexposed spot, at a laser power density of 350 mW cm^{-2}. At still lower laser irradiance, the trend did not change.

[e]At higher laser irradiance and time resolution, the trajectory would be increasingly stepwise.

[f]For QDs treated under the third condition, mild precipitations were seen. With the loss of the COO^- group, the QDs would be hydrophobic and would aggregate. Also see ref 5.

REFERENCES

(1) Michalet, X.; Pinaud, F. F.; Bentolila, L. A.; Tsay, J. M.; Doose, S.; Li, J. J.; Sundaresan, S.; Wu, A. M.; Gambhir, S. S.; Weiss, S. *Science* **2005**, *307*, 538−544.

(2) Qu, L. H.; Peng, X. G. *J. Am. Chem. Soc.* **2002**, *124*, 2049−2055.

(3) Chan, W. C. W.; Nie, S. *Science* **1998**, *281*, 2016−2018.

(4) Chen, Y.-J.; Yan, X.-P. *Small* **2009**, *5*, 2012−2018.

(5) Ma, J.; Chen, J.-Y.; Zhang, Y.; Wang, P.-N.; Guo, J.; Yang, W.-L.; Wang, C.-C. *J. Phys. Chem. B* **2007**, *111*, 12012−12016.

(6) Dabbousi, B. O.; RodriguezViejo, J.; Mikulec, F. V.; Heine, J. R.; Mattoussi, H.; Ober, R.; Jensen, K. F.; Bawendi, M. G. *J. Phys. Chem. B* **1997**, *101*, 9463−9475.

(7) Amelia, M.; Avellini, T.; Monaco, S.; Impellizzeri, S.; Yildiz, I.; Raymo, F. M.; Credi, A. *Pure Appl. Chem.* **2011**, *83*, 1−8.

(8) Gill, R.; Bahshi, L.; Freeman, R.; Willner, I. *Angew. Chem., Int. Ed.* **2008**, *47*, 1676−1679.

(9) Pellegrino, T.; Manna, L.; Kudera, S.; Liedl, T.; Koktysh, D.; Rpgach, A. L.; Keller, S.; Rädler, J.; Natile, G.; Parak, W. J. *Nano Lett.* **2004**, *4*, 703−707.

(10) Lee, Y. L.; Lo, Y. S. *Adv. Funct. Mater.* **2009**, *19*, 604−609.

(11) Chen, J.-Y.; Lee, Y.-M.; Zhao, D.; Mak, N.-K.; Wong, R. N.-S.; Chan, W.-H.; Cheung, N.-H. *Photochem. Photobiol.* **2010**, *18*, 431−437.

(12) Lee, S. F.; Osborne, M. A. *J. Am. Chem. Soc.* **2007**, *129*, 8936−8937.

(13) Durisic, N.; Godin, A. G.; Walter, D.; Grütter, P.; Wiseman, P. W.; Heyes, C. D. *ACS Nano* **2011**, *5*, 9062−9073.

(14) Cordes, D. B.; Gamsey, S.; Singaram, B. *Angew. Chem., Int. Ed.* **2006**, *45*, 3829−3832.

(15) Carrillo-Carrión, C.; Càrdenas, S.; Simonet, B. M.; Valcárcel, M. *Chem. Commun.* **2009**, 5214−5226.

(16) Sato, K.; Kojima, S.; Hattori, S.; Chiba, T.; Ueda-Sarson, K.; Torimoto, T.; Tachibana, Y.; Kuwabata, S. *Nanotechnology* **2007**, *18*, 465702.

(17) Kwok, K.-C.; Cheung, N.-H. *Anal. Chem.* **2010**, *82*, 3819−3825.

(18) Kwok, K.-C. Measuring Binding Kinetics of Ligands with Tethered Receptors by Fluorescence Polarization Complemented with Total Internal Reflection Fluorescence Microscopy. Ph.D. Thesis, Hong Kong Baptist University, 2010.

(19) Lakowicz, J. R. *Principles of Fluorescence Spectroscopy*, 3rd ed.; Springer: New York, 2006.

(20) Kwok, K. C.; Yeung, K. M.; Cheung, N. H. *Langmuir* **2007**, *23*, 1948−1952.

(21) Yeung, K. M. The Adsorption of Bovine Serum Albumin on Fused Silica: A Single Molecules Study. Ph.D. Thesis, Hong Kong Baptist University, 2008.

(22) Empedocles, S. A.; Neuhauser, R.; Bawendi, G. *Nature* **1999**, *399*, 126−130.

(23) Koberling, F.; Kolb, U.; Philip, G.; Potapova, I.; Basché, T.; Mews, A. *J. Phys. Chem. B* **2003**, *107*, 7463−7471.

(24) Invitrogen. Qdot Biotin Conjugates User Manual, Jan 2006. Downloadable from http://probes.invitrogen.com/media/pis/mp19003.pdf.

(25) Durisic, N.; Wiseman, P. W.; Grutter, P.; Heyes, C. D. *ACS Nano* **2009**, *3*, 1167−1175.

(26) Sperling, R. A.; Parak, W. J. *Philos. Trans. R. Soc. A* **2010**, *368*, 1333−1383.

(27) Adams, E. W.; Bruchez, M. P., Jr. US Patent 6,649,138 B2, 2003.

(28) Zhu, H.; Song, N.; Lian, T. *J. Am. Chem. Soc.* **2010**, *132*, 15038−15045.

(29) Gómez, D. E.; Califano, M.; Mulvaney, P. *Phys. Chem. Chem. Phys.* **2006**, *8*, 4989−5011.

(30) Impellizzeri, S.; Monaco, S.; Yildiz, I.; Amelia, M.; Credi, A.; Raymo, F. M. *J. Phys. Chem. C* **2010**, *114*, 7007−7013.

(31) Huang, B.; Bates, M.; Zhuang, X. *Annu. Rev. Biochem.* **2009**, *78*, 993−1016.